UC San Diego
UC San Diego Previously Published Works

Title

Near-Infrared-Induced Heating of Confined Water in Polymeric Particles for Efficient Payload Release

Permalink

https://escholarship.org/uc/item/5zq5x52d

Journal

ACS Nano, 8(5)

ISSN

1936-0851

Authors

Viger, Mathieu L

Sheng, Wangzhong

Doré, Kim

et al.

Publication Date

2014-05-27

DOI

10.1021/nn500702g

Near-Infrared-Induced Heating of Confined Water in Polymeric Particles for Efficient Payload Release

Mathieu L. Viger,[†,#] Wangzhong Sheng,[‡,#] Kim Doré,[§] Ali H. Alhasan,[†,∥] Carl-Johan Carling,[†] Jacques Lux,[†] Caroline de Gracia Lux,[†] Madeleine Grossman,[⊥] Roberto Malinow,[§] and Adah Almutairi[†,∥],*

[†]Skaggs School of Pharmacy and Pharmaceutical Sciences, [‡]Department of Mechanical and Aerospace Engineering, Materials Science and Engineering Program, [§]Center for Neural Circuits and Behavior, Division of Biology, Department of Neuroscience and Section of Neurobiology, [⊥]Department of Chemistry and Biochemistry, and [∥]KACST—UCSD Center of Excellence in Nanomedicine, University of California, San Diego, 9500 Gilman Drive, La Jolla, California 92093-0600, United States. [#]These authors contributed equally to this work.

ABSTRACT
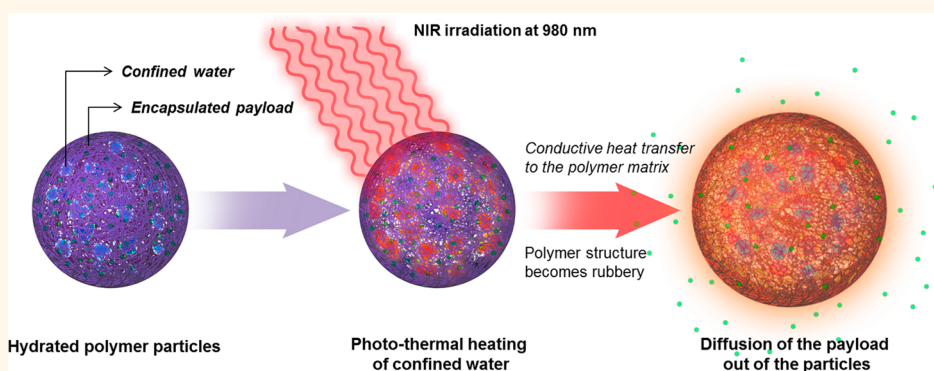
Near-infrared (NIR) light-triggered release from polymeric capsules could make a major impact on biological research by enabling remote and spatiotemporal control over the release of encapsulated cargo. The few existing mechanisms for NIR-triggered release have not been widely applied because they require custom synthesis of designer polymers, high-powered lasers to drive inefficient two-photon processes, and/or coencapsulation of bulky inorganic particles. In search of a simpler mechanism, we found that exposure to laser light resonant with the vibrational absorption of water (980 nm) in the NIR region can induce release of payloads encapsulated in particles made from inherently non-photo-responsive polymers. We hypothesize that confined water pockets present in hydrated polymer particles absorb electromagnetic energy and transfer it to the polymer matrix, inducing a thermal phase change. In this study, we show that this simple and highly universal strategy enables instantaneous and controlled release of payloads in aqueous environments as well as in living cells using both pulsed and continuous wavelength lasers without significant heating of the surrounding aqueous solution.

KEYWORDS: polymeric carriers · confined water · near-infrared radiation · photothermal effect · triggered release

Light-triggered release from polymeric particles is a key tool for delivering encapsulated molecules with a high degree of spatial and temporal control.[1−6] Given the deep penetration depth and low attenuation of near-infrared (NIR) radiation in biological tissues, systems that respond to these wavelengths (750−1300 nm) are particularly attractive.[7] Though many technologies facilitating release of encapsulated cargo from polymeric carriers using NIR radiation have been developed, all of them originate from only a handful of photochemical and photophysical strategies, which present drawbacks that limit the extent of their application. For example, gold or other metal nanostructures are often incorporated to generate heat upon absorption of NIR light, loosening the surrounding polymer matrix to release therapeutics.[8,9] This approach is limited by the controversial biocompatibility of metal nanostructures and the considerable amount of heat generated that may be detrimental to surrounding
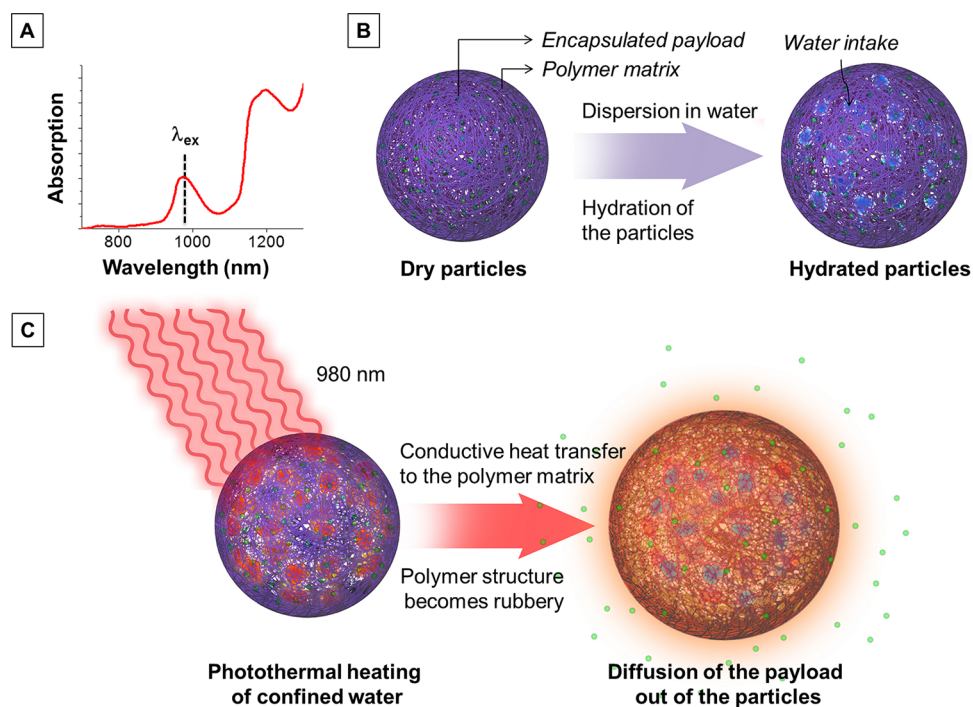
Figure 1. Schematic representation of NIR-induced release mechanism: (A) absorption spectrum of water in the NIR region; (B) formation of isolated nanodomains of water in the polymeric structure; (C) release of encapsulated molecules following photothermal heating of water droplets inside the polymer particles.

tissues.[10−12] Alternatively, carriers can also be formulated from polymers containing photoresponsive modalities that respond through chemical changes such as isomerization, oxidation, dimerization, and bond cleavage.[13,14] In order to make use of the inherently low energy of NIR light, these mechanisms all require simultaneous two-photon absorption, necessitating the use of high-powered and focused pulsed NIR lasers, with energies sometimes exceeding the damage threshold of biological tissue.[15,16] Recently, the limitations of two-photon photochemistry have been overcome by coupling photosensitive polymer carriers to upconverting nanoparticles (UCNPs) that sequentially absorb multiple NIR photons and convert them into higher-energy photons in the UV region.[17,18] Since excitation photons do not have to be absorbed simultaneously, UCNPs could enable triggered release in response to more biologically benign power densities. However, UCNPs contain heavy rare-earth elements that may prove to be toxic *in vitro* and *in vivo*.[19] These significant barriers to widespread application encourage further work to discover metal-free, universal strategies for remote-controlled photorelease using NIR light.

In search of such a mechanism, we found that exposure to NIR laser light resonant with the vibrational overtone of water at 980 nm (Figure 1A) could induce release of an encapsulated payload from particles made of inherently non-light-sensitive polymers, such as poly(lactic-*co*-glycolic acid) (PLGA). We hypothesize that this universal release mechanism arises from the interaction between the electromagnetic

radiation and confined nanodomains of water formed upon hydration of the particles (Figure 1B).[20,21] Upon exposure to 980 nm NIR light, water molecules absorb optical energy through vibrational transitions and the excitation energy is rapidly converted into heat.[22−24] In the case of bulk water, the heat is rapidly dissipated through the whole aqueous environment *via* convective heat transfer.[25] However, for small water droplets trapped inside polymer microstructures and partially shielded from the external bulk water, the absorption of resonant electromagnetic energy increases the internal droplets' temperature. To equilibrate the resulting temperature gradients, part of the generated heat is hypothesized to be lost by conductive heat transfer to the surrounding constituting matrix (Figure 1C), thus locally increasing the temperature of the polymer. Localized heating of the polymer matrix above the polymer's glass transition temperature would induces a phase change from a rigid, glassy state to a compliant, rubbery state, activating diffusion of encapsulated payload out of the particles.

Using real-time monitoring of steady-state fluorescence, we found that this strategy can be readily applied to precisely control the release of encapsulated contents of varying hydrophobicities from different polymer particles in aqueous environments as well as in living cells. We chose PLGA as the main polymer matrix because it is FDA-approved, widely used for a variety of biomaterials applications, and extensively studied as a drug carrier.[21,26] In the NIR region, water has vibrational absorption bands around 1950, 1450,
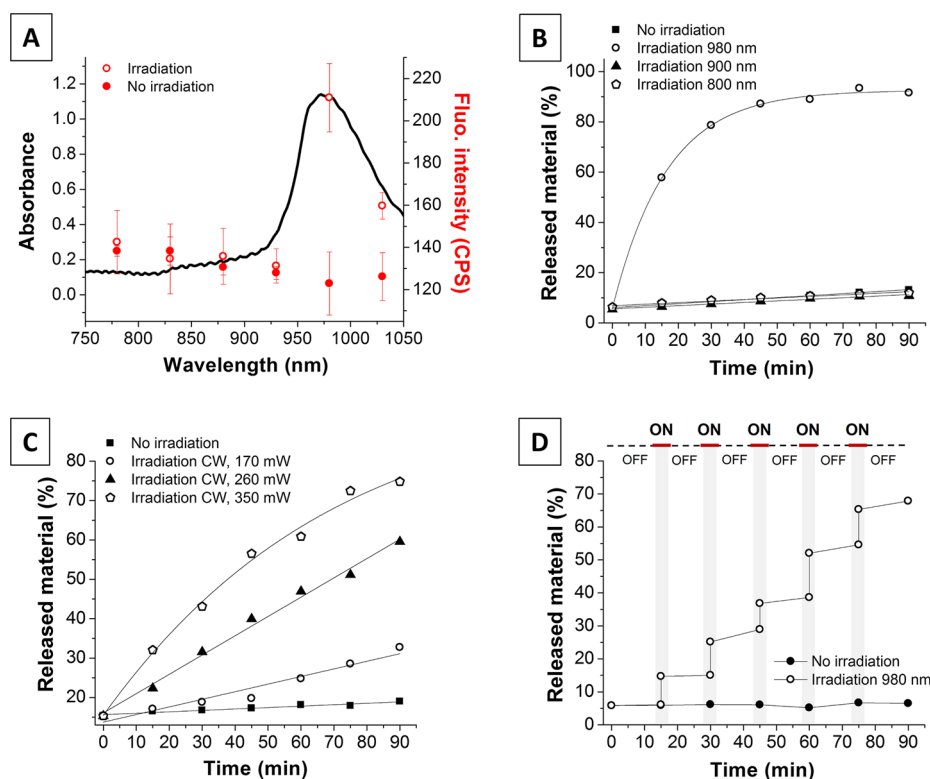
Figure 2. NIR-induced release occurs only at water-resonant wavelengths. (A) Action spectrum of the fluorescence intensity of a suspension of fluorescein-doped PLGA particles after 15 min irradiation (open circles) or 15 min at room temperature (solid circles) superimposed on the water absorption spectrum (black trace) ($N = 3$). (B) Cumulative fluorescein release after irradiation of a suspension of fluorescein-doped PLGA particles with pulsed laser light (1 W) at 980 nm (open circles), 900 nm (solid triangles), and 800 nm (open pentagons). Control (no irradiation, solid squares). (C) Cumulative fluorescein release after irradiation of a suspension of fluorescein-doped PLGA particles with 980 nm CW laser light at varying powers. (D) Stepwise triggered release from fluorescein-loaded PLGA particles using six cycles of nonirradiation (15 min) and five cycles of irradiation (5 min, 980 nm, pulsed laser, 1 W). Fluorescein acquisition parameters: $\lambda_{ex} = 480$ nm, $\lambda_{em} = 520$ nm.

1200, and 980 nm.[27] While the absorption coefficient increases at longer wavelengths, we chose 980 nm light for this study because wavelengths above 1100 nm were not readily available to us. However, the other overtone vibrational absorption bands should be capable of inducing release in a similar fashion. With fluorescence lifetime imaging microscopy (FLIM), we measured the temperature inside polymeric particles with high spatial resolution, which revealed increases in temperature upon irradiation at 980 nm. This simple and generalizable release mechanism represents a major innovation in the field of remote-controlled release, as it can be applied to a large number of systems with no inherent light sensitivity.

RESULTS AND DISCUSSION

NIR Irradiation at a Water-Resonant Wavelength Induces Payload Release from Polymeric Capsules. PLGA polymer capsules incorporating model compounds of varying hydrophobicities (fluorescein, Nile blue, Nile red, IR780) were produced by electrospray. Representative dark-field images and optical epifluorescence of the produced dye-loaded PLGA particles are shown in Figure S1 and Figure S2, respectively, in the Supporting Information. The wavelength selective response was first

explored by monitoring the change in fluorescence intensity of a suspension of fluorescein-loaded particles (size, 0.5 ± 0.1 μm; dye loading, ~10% w/w) before and after 15 min irradiation at 50 nm increments of wavelengths, ranging from 780 to 1030 nm (Figure 2A). Fluorescein emission increases upon release because it fluoresces more intensely in a polar environment and, like most organic dyes, self-quenches when its relative concentration exceeds ~10^{-3} M, such as when it is entrapped within particles (0.2 mol of fluorescein per kg of PLGA).[28] A strong increase in fluorescence intensity was obtained only when the irradiation wavelength coincided with the maximum water absorption band (i.e., 980 nm; Figure 2A, open circles); profiles following irradiation at nonresonant wavelengths were very similar to those of nonirradiated control samples (Figure 2A, solid circles). The rate of light-induced release of fluorescein was also monitored by fluorescence spectroscopy (see Methods section for experimental details). When excited at 980 nm (1 W), the amount of released material rapidly increased in the first 30 min and saturated at around 60 min (Figure 2B, open circles). The quantity of released material was found to be proportional to the amount of energy (number of photons) provided to

the system, where a cumulative 47, 76, and 89% of fluorescein, corresponding to 1.51 ± 0.06, 2.44 ± 0.01, and 2.84 ± 0.05 μg, was released from the PLGA particles after 10, 30, and 60 min of irradiation, respectively. Fluorescein release could be monitored visually as the suspension changed from colorless to bright green (Figure S3A). Epifluorescence microscopic images (Figure S3B) further confirmed NIR-triggered release: Before NIR irradiation, fluorescein was clearly loaded inside PLGA particles; after irradiation, fluorescence appeared as irregularly shaped dried patterns, rather than well-defined domains. In contrast, particles not exposed to light (off-state) or irradiated at nonresonant wavelengths (i.e., 800 and 900 nm) released negligible amounts of dye over the course of several minutes (Figure 2B). This wavelength selective response demonstrates the necessity of resonant photon interactions with water. The observed low background leakage of nonirradiated controls suggests that the fluorescein molecules remain well-encapsulated inside the PLGA particles. We calculated a 25-fold increase in the rate of fluorescein release upon exposure to 980 nm NIR light (on/off ratio).

SEM images of irradiated particles (Figure S4) showed no obvious changes in particle morphology (i.e., size, shape, and surface texture); even after 90 min of 980 nm pulsed irradiation at 1 W, no degradation was observed. To further confirm that 980 nm irradiation does not degrade the polymer, PLGA particles were run through gel permeation chromatography (GPC) before and after irradiation at 980 nm for 1 h (pulsed laser, 1 W). The GPC data did not show any change in retention time of the polymer and/or the appearance of small molecule peaks at longer retention times corresponding to products of degradation (Figure S5). As this mechanism induced release of the encapsulated payload without disruption of the polymer matrix, possible mechanisms such as optical cavitation or thermally induced ester degradation could be ruled out. More specifically, optical cavitation, or the formation of bubbles of vaporized gas in response to light, results from aqueous absorption of short laser pulses which generate a dielectric breakdown at the focal point, creating a plasma that expands and produces an acoustic shockwave.[29] Since laser-induced cavitation requires intense laser light (>200 nJ/pulse) focused at a spot size of 0.5−5 μm,[30] and laser beams with pulse energy ≤60 nJ and spot size diameters ≥2 mm were used in this release study, it is unlikely that the observed photorelease resulted from optical cavitation. Although no clear evidence of particle deformation was observed by SEM, irradiation did appear to reduce particle stability, as reflected by collapse and agglomeration (Figure S6). Aggregation could result from the particles being heated above their glass transition (T_g) and reaching a more rubbery state.[31,32] Nonetheless, the temperature increase of the bulk solution was less than a few degrees above ambient. We found that temperature elevations of the bulk solution from ambient temperature were dependent on laser power and sample volume. Irradiation at 980 nm (1 W, 15 min) of 0.25, 1, and 2 mL aliquots of a particle suspension resulted in maximum temperature elevations of approximately 10, 5, and 2 °C, respectively. In order to avoid unnecessary variability in the release experiments due to bulk heating, we can minimize temperature elevation of the bulk by working with large sample volumes.

As mentioned previously, the photophysical process involved in this release scheme occurs through the excitation of an overtone vibration absorption of water and so is not limited to delivery of 980 nm light as short, focused light pulses, in contrast to simultaneous two-photon absorption processes. Thus, efficient light-triggered release can also be achieved at lower excitation powers using a more economical and biologically relevant continuous wave (CW) laser setup (Figure 2C). By varying the excitation power from 170 to 350 mW, we found that the rate of release depends on the average photon energy used to excite PLGA particles. As expected, the release of fluorescein is faster at higher CW power, with an on/off ratio of 18 when irradiating at 350 mW compared to 14 and 5 when irradiating at 260 and 170 mW, respectively.

Since robust control over release is desired, we assessed the activatable nature of this release mechanism. A permanent effect would cause continuous release after irradiation ends, while an activatable effect would involve slowed release profiles following termination of laser irradiation.[33,34] A fluorescein-doped PLGA particle suspension was irradiated repeatedly using NIR light (pulsed laser, 980 nm, 1 W) for 5 min, followed by 15 min intervals with the laser turned off. A rapid increase in fluorescein release from the PLGA particles was observed upon NIR irradiation, but the release rate practically decreased to its initial rate when the NIR irradiation was switched off (Figure 2D). A similar on/off release ratio was observed over multiple consecutive exposures. This stepwise triggered release indicates that the PLGA particles retain their integrity upon NIR irradiation. The small payload release observed in the off-state may be attributed in part to water molecules diffusing into the space created by the loss of fluorescein from the particles, which in turn encourages outward diffusion.[20]

Since the PLGA particles are capable of encapsulating both hydrophobic and hydrophilic compounds at high efficiency, the ability of this photothermal process to release small payloads of varying hydrophobicities was investigated. IR780, Nile red, and Nile blue (in order of increasing polarity) were loaded by electrospray into spherical PLGA capsules (~10% w/w) of 0.7 ± 0.1, 1.4 ± 0.3, and 1.2 ± 0.4 μm in size, respectively (dark-field microscopy, Figure S1; fluorescence microscopy, Figure S2). For all aqueous suspensions of dye-loaded
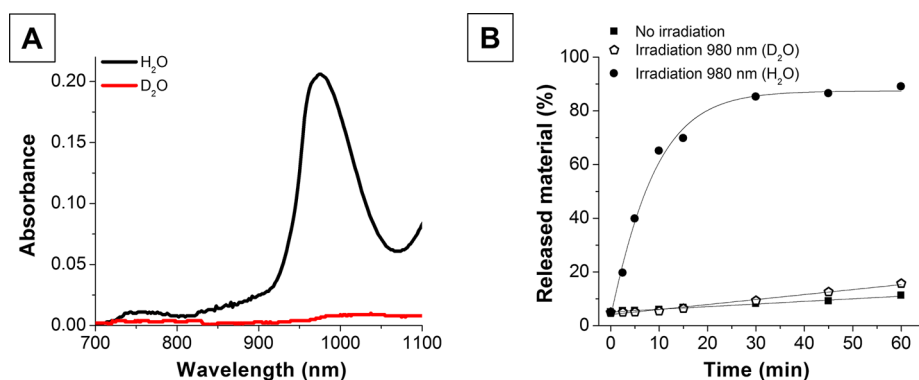
Figure 3. Metal-free photothermal release requires efficient vibrational absorption by confined water. (A) Absorption spectrum of deionized (H_2O) and deuterated water (D_2O). (B) Cumulative fluorescein release after irradiation of a suspension of fluorescein-doped PLGA particles dispersed H_2O (open circles) or D_2O (solid pentagons) with pulsed laser light at 980 nm. Control (no irradiation, solid squares). Laser power: 0.8 W.

PLGA particles, NIR exposure (980 nm, pulsed laser, 1 W) resulted in release of the dyes over time (Figure S7). These findings revealed that this photothermal process is capable of sustaining release of both hydrophilic and hydrophobic compounds. A noticeable trend in the kinetics of release related to differences in dye polarity could be observed; that is, more polar dyes were released faster. This difference could result from variations in water absorption: Hydrophilic content facilitates water penetration in polymeric carriers and leads to the creation of more porous and swelled polymer networks,[2] while more hydrophobic compounds hinder diffusion of water into the structure.[20,35] Variations in release rate could also relate to the energy needed to induce diffusion out of the matrix, which should be lower for hydrophilic than hydrophobic compounds since hydrophobic compounds would have higher affinity for the hydrophobic carrier. Also, as we have shown release with cargos that cannot be excited at 980 nm through two-photon absorption (Nile blue, IR780), the possibility that this light-assisted mechanism of release derives from thermal relaxation of two-photon excited states can be discarded.

Role of Water in Inducing Payload Release. In the proposed mechanism, entrapped water plays a crucial role in payload release by absorbing the NIR light to induce localized heating inside the particles. To test this hypothesis and rule out the possibility of direct absorption of optical energy by the polymer, we compared the release profiles of fluorescein from PLGA particles in deuterated water (D_2O) to those in deionized water (H_2O). A comparison of the absorption spectra of H_2O and D_2O shows that D_2O does not absorb significantly at 980 nm (Figure 3A). All of its vibrational transitions are shifted to lower energy by the increase in isotope mass; the vibrational band of H_2O at 980 nm is shifted to 1300 nm in D_2O.[36] Therefore, light-induced release in D_2O, if observed, could only be the result of photonic absorption by the polymer capsules. Fluorescein-loaded particles suspended in D_2O did not release cargo upon irradiation;

the kinetic profiles matched those of a nonirradiated sample (Figure 3B). This is consistent with previous results showing that the laser photonic densities (≤ 1 W) used in this study do not result in polymer degradation (Figure S5) and/or changes in PLGA particle morphology (Figure S4) and supports the conclusion that release requires strong absorbance of NIR light by water (Figure 2).

In the first stage of hydrolytic degradation, particles made of biodegradable polymers such as PLGA swell and take up water[20,21] to form domains of water in the hydrophobic nanostructure (Figure 1B).[37] While in this state, polymers' thermal behavior is affected, as the confined water acts as a plasticizer inside the polymer matrix by increasing the free volume of the polymer chains and consequently depressing the glass transition temperature (T_g); this process is called hydroplasticization.[38] Using differential scanning calorimetry (DSC), we measured the T_g of the PLGA particles before (dry T_g) and after dispersion in water (wet T_g). Based on the DSC measurements, the presence of a saturated water environment induced a depression of the T_g of PLGA particles from 42.6 to 27.9 °C, thus confirming the presence of water inside the capsules. The measured wet T_g value was in good agreement with the value predicted by a model proposed by Tsavalas et al.[38] (i.e., 27.1 °C), which we used to calculate a 5% water content weight fraction in the particles. PLGA carriers are complex 3D systems made of interconnecting pores and channels of different size and tortuosity distributed throughout the entire volume of the spheres in which water can penetrate rapidly.[39] Pre-existing pores (in contrast to dynamically formed pores created upon degradation) found in PLGA particles of similar composition and size present diameters between 3 and 20 nm;[39] water likely fills these pores.[40]

Since this mechanism of release relies on excitation of confined water, it should work on any polyester system without inherent light sensitivity at 980 nm. This versatility could have significant impact because linear polyesters (e.g., PLGA, poly(lactic acid), and

polycaprolactone) constitute one of the most important classes of synthetic biodegradable polymers[41,42] due to their biodegradability and biocompatibility, as well as their easily tailored physicochemical and mechanical properties.[43,44] We examined the applicability of this mechanism of release to other polyesters using Nile red-loaded polymer capsules (see inset in Figure S9 for molecular structures).[45] Fluorescence microscopy images of the resulting electrosprayed particles (polyester **1**, 0.9 ± 0.1 μm; polyester **2**, 2.3 ± 0.5 μm) can be found in Figure S8. For both aqueous suspensions of dye-loaded particles, NIR exposure (980 nm, pulsed laser, 0.9 W) resulted in release of the Nile red molecules over time (Figure S9). Both sets of particles presented similar stability in the absence of irradiation, suggesting that the confined water-assisted mechanism of release applies to multiple polyesters.[46]

Another important class of delivery vehicles are particles made from derivatized polysaccharides (*e.g.*, methacrylated hyaluronic acid,[47] chitosan,[48] and modified dextran[49,50]), which have attracted considerable attention for their tunable degradation rates, high processability, and biocompatible byproducts. To study the applicability of this photophysical mechanism to induce release from sugar-based polymers, we formulated Nile red-doped acetalated dextran particles using electrospray (size, 1.6 ± 0.5 μm; see Figure S8 for fluorescence microscopy images and size distribution histogram of the resulting particles) and tested the responsiveness of these particles to irradiation at 980 nm (pulsed laser, 0.9 W). Similarly to polyester particles, nonirradiated particles showed low background leakage (Figure S9C, solid squares), whereas irradiation at 980 nm induced a strong increase in payload release (Figure S9C, open circles). These results support the inference that remote-controlled photorelease using a water-resonant wavelength is applicable to a large number of systems with no inherent light sensitivity.

Evaluation of the Internal Temperature of the Particles upon 980 nm Irradiation. Fluorescent molecular thermometer represents a promising tool for intraparticle thermometry, as it functions at the molecular level and, thus, would be effective in monitoring temperature within micrometer-sized domains. The strong effect of temperature on the fluorescence of molecular probes has led to various sensing strategies based on changes in emission wavelength and/or fluorescence intensity.[51,52] In addition, excited-state lifetimes of fluorescent molecules are intensely affected by temperature, showing in most cases shorter lifetimes at higher temperatures.[53] This temperature dependence results from the increasing importance of nonradiative decay rates at higher temperatures. In this study, FLIM was used to extract intraparticle temperatures by comparing fluorescein lifetime to a standard curve generated by direct heating of the dye. This thermometric methodology allowed temperature measurements inside polymeric particles with high spatial and temperature resolution.

To image individual particles for an extended period of time, particles were stabilized in polyacrylamide hydrogels (see Methods). We first acquired a calibration curve relating free fluorescein lifetime and temperature by manually heating a polyacrylamide gel containing fluorescein from 20 °C (room temperature) to 70 °C and acquiring lifetime decay curves using a time-correlated single photon counting (TCSPC) system on a spectrofluorometer. The average excited-state decay times (τ_{av}) were then extracted (see Table S1) and plotted as lifetime change ($\Delta\tau_{av} = \tau_{av}(X\ °C) - \tau_{av}(20\ °C)$) as a function of temperature (Figure 4A). The excited-state lifetime deceased with increasing temperature following a negative linear relationship with a calculated sensitivity of −8 ps/°C. For the FLIM measurements, gels containing fluorescein-doped PLGA particles were placed in a reading chamber containing water. Single particles or small particle aggregates were irradiated at 980 nm (pulsed laser, 10 mW) in a raster scan motion to ensure complete irradiation of the entire particle/aggregate. FLIM images were acquired every 5 min, and an average lifetime was extracted from each image by integration of all pixels. Fluorescein's absorption/emission wavelengths and fluorescence lifetime are relatively insensitive to the environment's polarity; therefore, changes in lifetime recorded for the free dye in the hydrogel (Figure 5A) should correlate well to those recorded in the particles. Since fluorescein can be excited at 980 nm through two-photon absorption, the decay curves could be acquired while particles were continuously irradiated. Measurement of particle temperature *via* lifetime of encapsulated fluorescein would not otherwise be possible, as the particles' internal temperature equilibrates with that of the surrounding solution rapidly after irradiation. Lifetime measurements reveal increases in the lifetime of fluorescein within particles following cessation of irradiation (Figure S10).

The average lifetime of fluorescein within particles, as extracted from FLIM images, clearly decreases with increasing irradiation time (Figure 4B, open circles; see also Table S2 for lifetime data) ($\Delta\tau_{av} = -267 ± 31$ ps, $t_{irr} = 25$ min) following an exponential trend. According to the change in lifetime *versus* temperature calibration curve in Figure 4A, the average internal temperature of PLGA particles reached 34, 45, and 54 °C following 5, 15, and 25 min irradiation, respectively, well above the wet T_g of the dye-doped PLGA particles. On the other hand, the lifetime of free fluorescein embedded in polyacrylamide gels did not decrease upon irradiation (Figure 4B, solid circles; see also Table S3 for lifetime data). These data suggest that the absorbed optical energy can be efficiently dissipated throughout the bulk hydrogel, preventing excessive localized heating. The observed selective heating of polymeric particles *versus* the bulk aqueous environment can be
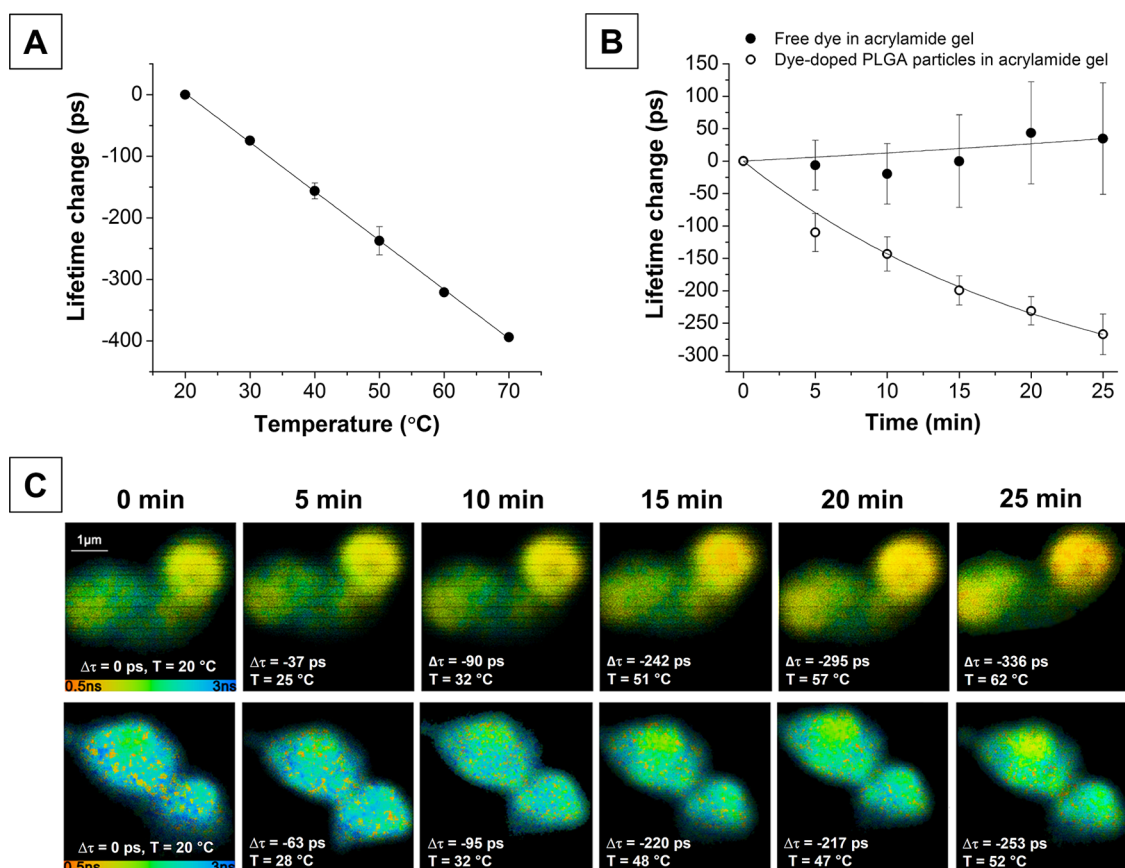
Figure 4. Fluorescence lifetime imaging reveals an increase in particles' internal temperature. (A) Change in average lifetime (ps) of free fluorescein in a polyacrylamide gel caused by heating to various temperatures. (B) Changes in average lifetime of free fluorescein in a polyacrylamide gel (solid circles) ($N = 4$) or encapsulated in PLGA particles and embedded in a polyacrylamide gel (open circles) ($N = 6$) upon irradiation at 980 nm (pulsed laser, 10 mW) for varying periods. (C) Two examples of FLIM images of fluorescein-doped PLGA particles embedded in a polyacrylamide gel after varying periods of irradiation at 980 nm (pulsed laser, 10 mW). The internal temperature was extracted from the calibration curve in (A).
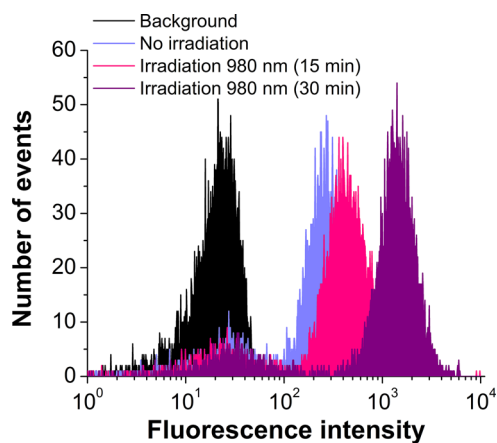

Figure 5. NIR-light-triggered intracellular FDA release. Background, cells incubated without particles; remaining traces, cells incubated with FDA-loaded particles and irradiated for varying periods. Irradiation, 980 nm; pulsed laser, 0.5 W.

attributed to the enormous volume difference between the two; the heat capacity of water within nanodomains is lower than that of bulk water. Also, it has been shown that water molecules confined in hydrophobic micro/nanostructures possess a much higher thermal conductivity than bulk water.[54] The space constraint causes an increase in collision frequency, which enhances energy and heat transfer.

Example FLIM images of small aggregates of particles within irradiated hydrogels show the consistency of decreasing fluorescein lifetime with increasing irradiation at 980 nm (Figure 4C). Though dye-doped particles presented different average lifetime values before irradiation (likely due to variations in particle size and dye loading), the change in lifetime of each particle as a function of irradiation time was comparable regardless of its initial value. These images also clearly show that thermal changes happened exclusively inside particles; no noticeable changes in the surrounding hydrogel were observed. Furthermore, because of the high spatial resolution of the FLIM system, regions of intense changes in lifetime were discernible throughout the whole polymer matrix, which suggested that water-rich areas capable of generating substantial heat were present within the PLGA particles. Using the relation found in Figure 4A, the corresponding average internal temperature was added to each FLIM image. These temperature

changes were more modest than in other thermally induced release mechanisms, especially compared to those involving gold nanostructures, which are reported to be well above 250 °C.[10,11] Compared to gold, for example, water has a much higher heat capacity (Cp, water = 4.186 J/g·°C; Cp, gold = 0.129 J/g·°C),[55] which means that it requires more optical energy to increase its temperature by the same amount. Ultimately, because the T_g of most biodegradable polymers is below 60 °C,[56] the resulting localized heating is enough to soften polymer matrices and induce release of the encapsulated payloads. An attractive option to increase the photon-to-heat conversion efficiency, and hence conserve the same release efficacy at lower laser powers, would be to exploit water absorption bands with greater absorptivity (i.e., 1200, 1450, and 1950 nm). This could prove especially useful for release experiments in highly scattering environments, as the laser beam would quickly broaden and lose its high peak power while traveling through the sample. Also, the polymeric capsules' sensitivity toward 980 nm excitation should be related to the amount of confined water in the polymeric capsules, which is greatly influenced by polymer composition (e.g., proportion of hydrophilic functionalities, potential to form intrapolymer hydrogen bonds, elastic modulus).[37,38] Thus, studying the effect of polymer composition (e.g., introducing hydrophilic functionalities) on particles' sensitivity to NIR light represents an exciting future direction and logical continuation of this work.

Light-Activated Intracellular Release. To examine whether this mechanism allows release of cargo from particles within cells, we first formulated polyester **1** particles (size = 0.7 ± 0.1 μm; see Figure S11 for dark-field microscopy and size distribution histogram) encapsulating the model release compound fluorescein diacetate (FDA). FDA is nonfluorescent in its native form but becomes highly fluorescent upon uptake by cells, as intracellular esterases hydrolyze the diacetate groups to produce fluorescein. Polyester **1** was chosen for these experiments because it possesses a glass transition in aqueous environments close to 37 °C (calculated wet T_g of 40 °C), which translates to less temperature-dependent release than PLGA (measured wet T_g of 28 °C). Particles were incubated with macrophages for 3 h, and cells were analyzed by flow cytometry following separation from free particles by centrifugation. Irradiation of cells incubated with FDA-loaded particles at 980 nm for 15 and 30 min resulted in 28- and 71-fold greater cell-associated fluorescence, respectively, than cells alone, while fluorescence increased by only 14-fold in nonirradiated cells (Figure 5). Not all cells took up FDA-loaded particles, as indicated by the left shoulder of the curves representing cells incubated with particles. The increase in released FDA with irradiation time, as indicated by fluorescence of its cleaved product, indicates tunable

control over the dose of cargo released. We believe that light-triggered FDA release is the result of heating of the confined water in the polyester particles because the increase in temperature of the bulk environment was minimal, from 37 ± 0.1 to 38.8 ± 0.1 °C after 30 min of irradiation (980 nm, pulsed laser, 0.5 W).

As irradiation at 980 nm could be harmful to cells, its effects on cell count and viability were measured. Upon exposure to 980 nm light (pulsed laser, 0.5 W, 30 min), no change in cell viability was observed (nonirradiated cells, 98.5 ± 0.6% viable; irradiated cells, 97.9 ± 0.6% viable; see Figure S12A) and only a slight decrease in cell density (19%) was detected (nonirradiated cells, 350 ± 10 cells/μL; irradiated cells, 290 ± 20 cells/μL; Figure S12B), which indicates that irradiation at this laser power causes minimal damage to living cells. The cytoxicity of the particles themselves has previously been reported as minimal up to a particle concentration of 100 μg/mL. These results demonstrate that 980 nm irradiation of polyester particles is a suitable means of triggering cargo release in living cells.

CONCLUSION

In the present study, we have demonstrated the feasibility of exploiting the unusual behavior of water confined within biodegradable polymeric particles to thermally induce a phase change upon NIR irradiation in polymer carriers with no inherent light sensitivity and achieve controlled release of an encapsulated payload in an aqueous environment and in living cells. This metal-free photoinduced release strategy involves (1) water diffusion into the polymer particles, (2) light-induced heating of confined water by targeting the overtone vibrational absorption band of water at 980 nm, (3) conductive heat transfer from the excited water droplets to the polymer matrix, (4) thermal phase change of the polymer particles to a more rubbery state, and (5) increase of the particles diffusivity and release of their encapsulated content. NIR light induced significant release of both hydrophilic and hydrophobic small molecules. The on-demand rate of release was found to depend on the average NIR photon energy administered to the system. Multiple consecutive NIR exposures can be used to obtain multiple release doses without irreversible rupture of the carriers and, given the high encapsulation efficiency of the electrospraying technique, allows a large number of release cycles. This new release mechanism provides additional benefits: wavelength selectivity and high sensitivity, which allows the use of low CW laser power and avoids excessive heating. With more research, we foresee multiple applications such as light-activated self-healing capsules, extracellular scaffolds (nanofibers, hydrogels) providing on-demand delivery of cues for cell proliferation, differentiation, or migration, activatable fluorescent particles based on thermochromic dyes, and light-triggered drug delivery

systems.[1,14,57] Given the successful demonstration of 980 nm laser-driven *in vivo* diagnosis[58−60] and therapy[61−63] at depths of several millimeters without excessive heat generation or tissue damage, we are hopeful that NIR-induced heating of particle-confined water may be widely adopted for site-specific photo-release in animal models, especially where light has direct access, for example, in the eye or optically transparent organisms such as *Caenorhabditis elegans* or zebrafish embryos.

METHODS

Materials. Poly(lactic-*co*-glycolic acid) (ratio 50:50; M_w 7−17 kDa; alkyl ester terminated), polystyrene (M_w 35 kDa), fluorescein (acid free, 95%), Nile blue chloride (85%), Nile red (technical grade), IR780 (98%), fluorescein diacetate (FDA), dextran (9−11 kDa), acrylamide (molecular biology grade), and N,N′-methylene bis(acrylamide) (99%) were purchased from Sigma-Aldrich. Pluronic F127 (13 kDa) was purchased from O-BASF. Lithium acylphosphinate salt was synthesized according to a procedure published by Fairbanks *et al.*[63] Dextran was acetalated according to a procedure described by Suarez *et al.*[64] The synthesis of polyesters **1** and **2** can be found elsewhere.[45] Chloroform (CHCl₃, 99.8%, EMD), dimethylformamide (DMF, 99%, Aldrich), tetrahydrofuran (THF, 99%, Fischer Scientific), and deuterated water (D 99.9%, Cambridge Isotope Inc.) were used without further purification. Deionized water (DI H₂O) was purified from a Millipore system (18.2 MΩ).

Preparation and Characterization of Polymer Particles. The polymer capsules incorporating model release compounds were produced by electrospray. This formulation method employs high voltages to inject charge into a liquid, causing the liquid to break into a jet of fine aerosol droplets propelled toward a metal plate collector. As the solvent evaporates in flight, dense, solid polymer particles are generated.[65] A variety of parameters, such as applied voltage, solution injection rate, and plate collector height, can be tuned to control the size and morphology of the particles.[66] This versatile method yields highly reproducible particles and entraps payloads at high encapsulation efficiencies. The dye-doped particles were obtained as follows: For most formulations, the polymer (100 mg) was dissolved in 0.75 mL of CHCl₃ and diluted with a solution containing the active compound in DMF (40 mg/mL, 0.25 mL) at 10% w/v. The prepared solutions were electrosprayed at 20 kV (Gamma High Voltage, ES30) at a flow rate of 0.5 mL/h (KD Scientific) using a 25 gauge needle. However, for polyester **1** particles encapsulating FDA molecules, 35 mg of the polymer was mixed with 3.5 mg of FDA and dissolved in 0.5 mL of 3:1 DMF/THF (7% w/v). This solution was electrosprayed at 28 kV (Gamma High Voltage, ES30) at a flow rate of 0.1 mL/h (KD Scientific) using a 25 gauge needle. The duration of the spray was kept the same between samples in order to yield the same final electrosprayed mass of polymer. Samples were collected onto microscope glass slides on an aluminum plate collector at a distance of 30 cm. The particles (∼2 mg) were removed from their glass slide substrate by sonication in DI H₂O, washed with DI H₂O, and finally dispersed in 5 mL of DI H₂O.

The morphology of the polymer particles was examined by fluorescence microscopy (Nikon, Eclipse, NIS Elements software) and SEM (Agilent, 8500). Particle diameter distributions were extracted from recorded fluorescence images and SEM photographs using NIS Elements (Nikon) and ImageJ software (NIH). The degree of polymer degradation induced by irradiation at 980 nm was studied by gel permeation chromatography (Waters), comparing a particle solution exposed to NIR light (980 nm, pulsed laser, 1 W) for 1 h to an nonirradiated sample. The amount of dye incorporated into the various particle samples was determined by dissolving the particles with CHCl₃ to release the dye from the particles. Fluorescein- and Nile blue-loaded PLGA particles (5 mL, 0.4 mg/mL) were solubilized in 0.5 mL of CHCl₃ first and then diluted in DI H₂O to a volume of 50 mL, whereas Nile red- and IR780-loaded PLGA particles were completely solubilized in 50 mL of CHCl₃. The fluorescence of the mixtures was measured and the dye concentration quantified by linear calibration with matrix-matched standards. Steady-state fluorescence measurements were performed using a Fluorolog spectrofluorimeter (Horiba Jobin-Yvon) and quartz cuvette (volume = 1.5 mL, optical path length = 1.0 cm). Differential scanning calorimetry (PerkinElmer DSC-7) was used to measure the glass transition temperatures of PLGA.

Release Experiments in Aqueous Environment. In a typical experiment, release from polymer particles was photoinitiated by irradiating aliquots (0.4 mg/mL) in a micro quartz cuvette at 50 nm increments from 780 to 1030 nm, for specified periods of time using either a Ti:sapphire laser (Mai Tai HP, Spectra Physics, 100 fs pulse width, 80 MHz repetition rate, 1 W, beam diameter = 2 mm) or a CW laser diode (Thorlabs, 980 nm only, 170−350 mW, beam diameter = 2 mm). A wave plate/polarizer combination was used to ensure an equal output power at 980, 900, and 800 nm. Release of the dyes was followed by fluorescence spectroscopy, and an emission spectrum was recorded immediately after every irradiation period. The release experiments regarding the hydrophilic dyes (fluorescein, Nile blue) were performed in pure water, whereas for the hydrophobic dyes (Nile red, IR780), a surfactant (pluronic F127, 0.1% w/v) was added to the particle solutions to establish a sink condition to facilitate release. The morphology of the irradiated particles was investigated by optical microscopy and SEM. Solution temperatures were measured using a thin wire thermocouple (J-Kem Scientific) immersed in the particle solutions while irradiating with the NIR light sources and connected to a temperature controller (J-Kem Scientific). Digital photographs were acquired using a Panasonic DMC-ZS5. The fraction of released material was quantified using fluorescence spectroscopy. Typically, after varying periods of irradiation, irradiated samples and nonirradiated controls were spun down (4500 rpm, 15 min) to separate the released material in the supernatant from the payload still encapsulated in the particles. The supernatant and particle pellet were dried (rotovap, vacuum) and subsequently dissolved in organic solvent (CHCl₃ or DMF). The fluorescence spectra were acquired, and the fluorescence intensity of the supernatant was compared to the total fluorescence intensity (*i.e.*, supernatant and particle pellet) to obtain the percentage of released material. The dye concentration was quantified by linear calibration with standards.

Nanoparticle Uptake and Photocontrolled Release in Cells. MV-4-11 (ATCC CRL-9591) human lymphoblast macrophage cells from peripheral blood were purchased from ATCC and cultured in Iscove's modified Eagle's medium (IMEM) supplemented with 10% fetal bovine serum. Cells were cultured in suspension and passaged three times before the experiment. Cells (5 × 10⁵/mL) were incubated at 37 °C, 5% CO₂, with FDA-loaded polyester **1** particles (100 μg/mL) suspended in IMEM for 3 h to accomplish cellular uptake. The cells were then isolated by centrifugation and washed three times with IMEM to remove particles that were not internalized and remained free in media. To induce intracellular release and subsequent hydrolysis of FDA molecules, aliquots (100 μL) of cells containing FDA-loaded particles were irradiated at 980 nm (pulsed laser, 0.5 W) for 15 and 30 min to maximize exposure of the sample to the laser. The sample was subsequently diluted 8-fold and quantified using a Guava EasyCyte flow cytometer (Millipore). Nonirradiated cells incorporating FDA-loaded particles were similarly prepared and analyzed as a control to probe the effect of nonspecific FDA release, whereas cells incubated without polymeric particles were used to set the background threshold. A commercial cell viability assay (Guava ViaCount, Millipore) was performed on nonirradiated and irradiated cell suspensions (980 nm, pulsed

laser, 0.5 W, 30 min), 48 h post-irradiation to determine the effect of the laser on cells.

Internal Temperature Measurement Using Fluorescence Lifetime. All lifetime experiments were performed on fluorescein-doped particles or free dye embedded in polyacrylamide gels. The hydrogels containing the particles were obtained by mixing a 250 μL particle aliquot (0.4 mg/mL) with acrylamide (60 mg), bis(acrylamide) (1.4 mg), and lithium acylphosphinate salt (58 mg/mL, 10 μL). The gelation was photoinitiated under UV irradiation (30 s, Luzchem). To obtain the free dye embedded in hydrogels, 250 μL of fluorescein-doped PLGA particle aliquot (0.4 mg/mL) was first heated at 65 °C for 15 min to release the dye molecules from the PLGA particles, and the empty polymer particles were removed by centrifugation before applying the same gelling process.

Fluorescence lifetime spectroscopy was done using a time-correlated single photon counting (TCSPC) system (Horiba) equipped with a NanoLED excitation source (488 nm, 1 MHz impulse repetition rate, Horiba) and a R928P detector (Hamamatsu Photonics, Japan). The detector was set to 520 nm for detection of fluorescein. The slit width varied between 2 and 20 nm to achieve an appropriate count rate. The instrument response function (IRF) was obtained by using a scattering solution of Ludox-40 (Sigma-Aldrich) in water (prompt) at 480 nm emission. The samples and the prompt were measured in a semimicro quartz cuvette. The lifetime was recorded on a 450 ns scale. A total of 4094 channels were used with a time calibration of 0.110 channel/ns. All decay curves were fitted with one exponential. The fluorescence lifetimes were extracted using DAS6 v6.6 decay analysis software (Horiba). The goodness of fit was judged by χ^2 values, Durbin–Watson parameters, and visual observation of the fit line and residuals, which should be distributed randomly about zero.

Fluorescence lifetime imaging was performed on a Slice-Scope two-photon microscope (Scientifica, UK) using a 60× water immersion objective (LUMPLFLN 60XW, NA = 1.0, Olympus). A Chameleon Ultra II IR laser (Coherent) (80 MHz repetition rate, 100–150 fs pulses) tuned at 980 nm was used for the excitation of both fluorescein and confined water. ScanImage r3.8 was used to control the scanning mirrors.[67] Fluorescence emission was detected with a hybrid PMT detector (HPM-100-40, Becker and Hickl, Germany) between 490 and 540 nm by means of a GFP emission filter (ET 515/50, Chroma). The acquisition of fluorescence lifetimes was synchronized by a TCSPC module (SPC-150, Becker and Hickl). The following parameters were kept constant for all acquired images: pixel size (30 nm; all 512 × 512 pixels), pixel dwell time (3.2 μs), laser excitation intensity (10 mW after the microscope objective), and FLIM acquisition time (60 s/image). Fluorescence lifetime images were analyzed with SPCimage (Becker and Hickl). To minimize lifetime calculation errors, we used a minimum threshold of 15 photons at the peak (corresponding to ~1000 photons per pixel) and a binning factor between 2 and 10 pixels to ensure sufficient photons in the regions of interest. The same calculated IRF was used for all experiments. The control images of free fluorescein in polyacrylamide gels were analyzed with a single exponential model, whereas the PLGA particle images were much better fitted with a double exponential model. The goodness of fit was evaluated with χ^2 values and visual observation of the fit line and residuals.

Conflict of Interest: The authors declare no competing financial interest.

Supporting Information Available: SEM images, fluorescence microscopic images, particle size distributions of the electrosprayed particles, release profiles, cytotoxicity, and lifetime data. Photographs of a particle suspension before and after irradiation. Fluorescence release experiments. This material is available free of charge *via* the Internet at http://pubs.acs.org.

REFERENCES AND NOTES

1. Esser-Kahn, A. P.; Odom, S. A.; Sottos, N. R.; White, S. R.; Moore, J. S. Triggered Release from Polymer Capsules. *Macromolecules* **2011**, *44*, 5539–5553.
2. Johnston, A. P. R.; Such, G. K.; Caruso, F. Triggering Release of Encapsulated Cargo. *Angew. Chem., Int. Ed.* **2010**, *49*, 2664–2666.
3. Timko, B. P.; Dvir, T.; Kohane, D. S. Remotely Triggerable Drug Delivery Systems. *Adv. Mater.* **2010**, *22*, 4925–4943.
4. Wang, G.; Tong, X.; Zhao, Y. Preparation of Azobenzene-Containing Amphiphilic Diblock Copolymers for Light-Responsive Micellar Aggregates. *Macromolecules* **2004**, *37*, 8911–8917.
5. Shum, P.; Kim, J. M.; Thompson, D. H. Phototriggering of Liposomal Drug Delivery Systems. *Adv. Drug Delivery Rev.* **2001**, *53*, 273–284.
6. Anderson, V. C.; Thompson, D. H. Triggered Release of Hydrophilic Agents from Plasmologen Liposomes Using Visible Light or Acid. *Biochim. Biophys. Acta, Biomembr.* **1992**, *1109*, 33–42.
7. Weissleder, R. A Clearer Vision for *In Vivo* Imaging. *Nat. Biotechnol.* **2001**, *19*, 316–317.
8. Hribar, K. C.; Lee, M. H.; Lee, D.; Burdick, J. A. Enhanced Release of Small Molecules from Near-Infrared Light Responsive Polymer–Nanorod Composites. *ACS Nano* **2011**, *5*, 2948–2956.
9. Wu, G.; Mikhailovsky, A.; Khant, H. A.; Fu, C.; Chiu, W.; Zasadzinski, J. A. Remotely Triggered Liposome Release by Near-Infrared Light Absorption *via* Hollow Gold Nanoshells. *J. Am. Chem. Soc.* **2008**, *130*, 8175–8177.
10. Radt, B.; Smith, T. A.; Caruso, F. Optically Addressable Nanostructured Capsules. *Adv. Mater.* **2004**, *16*, 2184–2189.
11. Wu, G.; Mikhailovsky, A.; Khant, H. A.; Zasadzinski, J. A. Synthesis, Characterization, and Optical Response of Gold Nanoshells Used To Trigger Release from Liposomes. *Methods Enzymol.* **2009**, *464*, 279–307.
12. Zhang, X. D.; Wu, D.; Shen, X.; Liu, P. X.; Fan, F. Y.; Fan, S. J. *In Vivo* Renal Clearance, Viodistribution, Toxicity of Gold Nanoclusters. *Biomaterials* **2012**, *33*, 4628–4638.
13. Olejniczak, J.; Sankaranarayanan, J.; Viger, M. L.; Almutairi, A. Highest Efficiency Two-Photon Degradable Copolymer for Remote Controlled Release. *ACS Macro Lett.* **2013**, *2*, 683–687.
14. Fomina, N.; Sankaranarayanan, J.; Almutairi, A. Photochemical Mechanisms of Light-Triggered Release from Nanocarriers. *Adv. Drug Delivery Rev.* **2012**, *64*, 1005–1020.
15. Koester, H. J.; Baur, D.; Uhl, R.; Hell, S. W. Ca^{2+} Fluorescence Imaging with Pico- and Femtosecond Two-Photon Excitation: Signal and Photodamage. *Biophys. J.* **1999**, *77*, 2226–2236.
16. Konig, K.; Becker, T. W.; Fischer, P.; Riemann, I.; Halbhuber, K. J. Pulse-Length Dependence of Cellular Response to Intense Near-Infrared Laser Pulses in Multiphoton Microscopes. *Opt. Lett.* **1999**, *24*, 113–115.
17. Carling, C.-J.; Nourmohammadian, F.; Boyer, J.-C.; Branda, N. R. Remote-Control Photorelease of Caged Compounds Using Near-Infrared Light and Upconverting Nanoparticles. *Angew. Chem., Int. Ed.* **2010**, *49*, 3782–3785.
18. Viger, M. L.; Grossman, M.; Fomina, N.; Almutairi, A. Low Power Upconverted Near-IR Light for Efficient Polymeric Nanoparticle Degradation and Cargo Release. *Adv. Mater.* **2013**, *25*, 3733–3738.
19. Choi, H. S.; Liu, W.; Misra, P.; Tanaka, E.; Zimmer, J. P.; Ipe, B. I.; Bawendi, M. G.; Frangioni, J. V. Renal Clearance of Quantum Dots. *Nat. Biotechnol.* **2007**, *25*, 1165–1170.

20. Engineer, C.; Parikh, J.; Raval, A. Review on Hydrolytic Degradation Behavior of Biodegradable Polymers from Controlled Drug Delivery System. *Trends Biomater. Artif. Organs* **2011**, *25*, 79–85.

21. Makadia, H. K.; Siegel, S. J. Poly Lactic-*co*-Glycolic Acid (PLGA) as Biodegradable Controlled Drug Delivery Carrier. *Polymers* **2011**, *3*, 1377–1397.

22. Tabakoglu, H. O.; Topaloglu, N.; Gulsoy, M. The Effect of Irradiance Level in 980-nm Diode Laser Skin Welding. *Photomed. Laser Surg.* **2010**, *28*, 453–458.

23. Zhan, Q. Q.; Qian, J.; Liang, H. J.; Somesfalean, G.; Wang, D.; He, S. L.; Zhang, Z. G.; Andersson-Engels, S. Using 915 nm Laser Excited Tm^{3+}/Er^{3+}/Ho^{3+}-Doped NaYbF$_4$ Upconversion Nanoparticles for *In Vitro* and Deeper *In Vivo* Bioimaging without Overheating Irradiation. *ACS Nano* **2011**, *5*, 3744–3757.

24. Gulsoy, M.; Dereli, Z.; Tabakoglu, H. O.; Bozkulak, O. Closure of Skin Incisions by 980-nm Diode Laser Welding. *Lasers Med. Sci.* **2006**, *21*, 5–10.

25. Park, B. S.; Armstrong, R. L. Laser Droplet Heating—Fast and Slow Heating Regimes. *Appl. Opt.* **1989**, *28*, 3671–3680.

26. Fredenberg, S.; Wahlgren, M.; Reslow, M.; Axelsson, A. The Mechanisms of Drug Release in Poly(lactic-*co*-glycolic acid)-Based Drug Delivery Systems—A Review. *Int. J. Pharm.* **2011**, *415*, 34–52.

27. Hale, G. M.; Querry, M. R. Optical Constants of Water in the 200-nm to 200-μm Wavelength Region. *Appl. Opt.* **1973**, *12*, 555–563.

28. Viger, M. L.; Live, L. S.; Therrien, O. D.; Boudreau, D. Reduction of Self-Quenching in Fluorescent Silica-Coated Silver Nanoparticles. *Plasmonics* **2008**, *3*, 33–40.

29. Abraham, E.; Minoshima, K.; Matsumoto, H. Femtosecond Laser-Induced Breakdown in Water: Time-Resolved Shadow Imaging and Two-Color Interferometric Imaging. *Opt. Commun.* **2000**, *176*, 441–452.

30. Glezer, E. N.; Schaffer, C. B.; Nishimura, N.; Mazur, E. Minimally Disruptive Laser-Induced Breakdown in Water. *Opt. Lett.* **1997**, *22*, 1817–1819.

31. De, S.; Robinson, D. H. Particle Size and Temperature Effect on the Physical Stability of PLGA Nanospheres and Microspheres Containing Bodipy. *AAPS PharmSciTech* **2004**, *5*, 18–24.

32. Friess, W.; Schlapp, M. Release Mechanisms from Gentamicin Loaded Poly(lactic-*co*-glycolic acid) (PLGA) Microparticles. *J. Pharm. Sci.* **2002**, *91*, 845–855.

33. de Gracia Lux, C.; McFearin, C. L.; Joshi-Barr, S.; Sankaranarayanan, J.; Fomina, N.; Almutairi, A. Single UV or Near IR Triggering Event Leads to Polymer Degradation into Small Molecules. *ACS Macro Lett.* **2012**, *1*, 922–926.

34. Fomina, N.; McFearin, C.; Sermsakdi, M.; Edigin, O.; Almutairi, A. UV and Near-IR Triggered Release from Polymeric Nanoparticles. *J. Am. Chem. Soc.* **2010**, *132*, 9540–9542.

35. Siegel, S. J.; Kahn, J. B.; Metzger, K.; Winey, K. I.; Werner, K.; Dan, N. Effect of Drug Type on the Degradation Rate of PLGA Matrices. *Eur. J. Pharm. Biopharm* **2006**, *64*, 287–293.

36. Bayly, J. G.; Kartha, V. B.; Stevens, W. H. The Absorption Spectra of Liquid Phase H$_2$O, HDO and D$_2$O from 0.7 μm to 10 μm. *Infrared Phys.* **1963**, *3*, 211–222.

37. Lei, Y.; Child, J. R.; Tsavalas, J. G. Design and Analysis of the Homogeneous and Heterogeneous Distribution of Water Confined within Colloidal Polymer Particles. *Colloid Polym. Sci.* **2013**, *291*, 143–156.

38. Tsavalas, J. G.; Sundberg, D. C. Hydroplasticization of Polymers: Model Predictions and Application to Emulsion Polymers. *Langmuir* **2010**, *26*, 6960–6966.

39. Sandor, M.; Enscore, D.; Weston, P.; Mathiowitz, E. Effect of Protein Molecular Weight on Release from Micron-Sized PLGA Microspheres. *J. Controlled Release* **2001**, *76*, 297–311.

40. Zhao, A. Y.; Hunter, S. K.; Rodgers, V. G. J. Theoretical Prediction of Induction Period from Transient Pore Evolvement in Polyester-Based Microparticles. *J. Pharm. Sci.* **2010**, *99*, 4477–4487.

41. Ikada, Y.; Tsuji, H. Biodegradable Polyesters for Medical and Ecological Applications. *Macromol. Rapid Commun.* **2000**, *21*, 117–132.

42. Ihre, H. R.; De Jesus, O. L. P.; Szoka, F. C.; Frechet, J. M. J. Polyester Dendritic Systems for Drug Delivery Applications: Design, Synthesis, and Characterization. *Bioconjugate Chem.* **2002**, *13*, 443–452.

43. Mohamed, F.; van der Walle, C. F. Engineering Biodegradable Polyester Particles with Specific Drug Targeting and Drug Release Properties. *J. Pharm. Sci.* **2008**, *97*, 71–87.

44. Breitenbach, A.; Li, Y. X.; Kissel, T. Branched Biodegradable Polyesters for Parenteral Drug Delivery Systems. *J. Controlled Release* **2000**, *64*, 167–178.

45. de Gracia Lux, C.; Joshi-Barr, S.; Nguyen, T.; Mahmoud, E.; Schopf, E.; Fomina, N.; Almutairi, A. Biocompatible Polymeric Nanoparticles Degrade and Release Cargo in Response to Biologically Relevant Levels of Hydrogen Peroxide. *J. Am. Chem. Soc.* **2012**, *134*, 15758–15764.

46. Vert, M. Aliphatic Polyesters: Great Degradable Polymers That Cannot Do Everything. *Biomacromolecules* **2005**, *6*, 538–546.

47. Messager, L.; Portecop, N.; Hachet, E.; Lapeyre, V.; Pignot-Paintrand, I.; Catargi, B.; Auzely-Velty, R.; Ravaine, V. Photochemical Crosslinking of Hyaluronic Acid Confined in Nanoemulsions: Towards Nanogels with a Controlled Structure. *J. Mater. Chem. B* **2013**, *1*, 3369–3379.

48. Bhattarai, N.; Gunn, J.; Zhang, M. Q. Chitosan-Based Hydrogels for Controlled, Localized Drug Delivery. *Adv. Drug Delivery Rev.* **2010**, *62*, 83–99.

49. Broaders, K. E.; Cohen, J. A.; Beaudette, T. T.; Bachelder, E. M.; Frechet, J. M. J. Acetalated Dextran Is a Chemically and Biologically Tunable Material for Particulatel. *Proc. Natl. Acad. Sci. U.S.A.* **2009**, *106*, 5497–5502.

50. Broaders, K. E.; Grandhe, S.; Frechet, J. M. J. A Biocompatible Oxidation-Triggered Carrier Polymer with Potential in Therapeutics. *J. Am. Chem. Soc.* **2011**, *133*, 756–758.

51. Chapman, C. F.; Liu, Y.; Sonek, G. J.; Tromberg, B. J. The Use of Exogenous Fluorescent-Probes for Temperature-Measurements in Single Living Cells. *Photochem. Photobiol.* **1995**, *62*, 416–425.

52. Brites, C. D.; Lima, P. P.; Silva, N. J.; Millan, A.; Amaral, V. S.; Palacio, F.; Carlos, L. D. A Luminescent Molecular Thermometer for Long-Term Absolute Temperature Measurements at the Nanoscale. *Adv. Mater.* **2010**, *22*, 4499–504.

53. Lakowicz, J. R. *Principles of Fluorescence Spectroscopy*; Springer: London, 1983.

54. Liu, Y. C.; Wang, Q. Transport Behavior of Water Confined in Carbon Nanotubes. *Phys. Rev. B* **2005**, *72*, 085420/1–085420/4.

55. Weast, R. C. *CRC Handbook Chem. Physics*, 1st student ed.; CRC Press: Boca Raton, FL, 1988.

56. Middleton, J. C.; Tipton, A. J. Synthetic Biodegradable Polymers as Orthopedic Devices. *Biomaterials* **2000**, *21*, 2335–2346.

57. Blaiszik, B. J.; Kramer, S. L. B.; Olugebefola, S. C.; Moore, J. S.; Sottos, N. R.; White, S. R. Self-Healing Polymers and Composites. *Annu. Rev. Mater. Res.* **2010**, *40*, 179–211.

58. Naczynski, D. J.; Tan, M. C.; Zevon, M.; Wall, B.; Kohl, J.; Kulesa, A.; Chen, S.; Roth, C. M.; Riman, R. E.; Moghe, P. V. Rare-Earth-Doped Biological Composites as *In Vivo* Shortwave Infrared Reporters. *Nat. Commun.* **2013**, *4:2199*, 1–10.

59. Hong, G. S.; Lee, J. C.; Robinson, J. T.; Raaz, U.; Xie, L. M.; Huang, N. F.; Cooke, J. P.; Dai, H. J. Multifunctional *In Vivo* Vascular Imaging Using Near-Infrared II Fluorescence. *Nat. Med.* **2012**, *18*, 1841–1846.

60. Liu, Q.; Sun, Y.; Yang, T. S.; Feng, W.; Li, C. G.; Li, F. Y. Sub-10 nm Hexagonal Lanthanide-Doped NaLuF$_4$ Upconversion Nanocrystals for Sensitive Bioimaging *in Vivo*. *J. Am. Chem. Soc.* **2011**, *133*, 17122–17125.

61. Dong, K.; Liu, Z.; Li, Z. H.; Ren, J. S.; Qu, X. G. Hydrophobic Anticancer Drug Delivery by a 980 nm Laser-Driven Photothermal Vehicle for Efficient Synergistic Therapy of Cancer Cells *in Vivo*. *Adv. Mater.* **2013**, *25*, 4452–4458.

62. Jayakumar, M. K. G.; Idris, N. M.; Zhang, Y. Remote Activation of Biomolecules in Deep Tissues Using Near-Infrared-to-UV Upconversion Nanotransducers. *Proc. Natl. Acad. Sci. U.S.A.* **2012**, *109*, 8483–8488.

63. Fairbanks, B. D.; Schwartz, M. P.; Bowman, C. N.; Anseth, K. S. Photoinitiated Polymerization of PEG-Diacrylate with Lithium Phenyl-2,4,6-trimethylbenzoylphosphinate: Polymerization Rate and Cytocompatibility. *Biomaterials* **2009**, *30*, 6702–6707.

64. Suarez, S.; Grover, G. N.; Braden, R. L.; Christman, K. L.; Amutairi, A. Tunable Protein Release from Acetalated Dextran Microparticles: A Platform for Delivery of Protein Therapeutics to the Heart Post-MI. *Biomacromolecules* **2013**, *14*, 3927–3935.

65. Bock, N.; Woodruff, M. A.; Hutmacher, D. W.; Dargaville, T. R. Electrospraying, a Reproducible Method for Production of Polymeric Microspheres for Biomedical Applications. *Polymers (Basel, Switz.)* **2011**, *3*, 131–149.

66. Almeria, B.; Deng, W.; Fahmy, T. M.; Gomez, A. Controlling the Morphology of Electrospray-Generated PLGA Microparticles for Drug Delivery. *J. Colloid Interface Sci.* **2010**, *343*, 125–133.

67. Pologruto, T. A.; Sabatini, B. L.; Svoboda, K. ScanImage: Flexible Software for Operating Laser Scanning Microscopes. *Biomed. Eng. Online* **2003**, *2*, 13.